

## The Automatic Calibration Unit in JUNO

---

Jiaqi Hui,<sup>a</sup> Hancheng Liu,<sup>b</sup> Jianglei Liu,<sup>a,c</sup> Yue Meng,<sup>a</sup> Mengjiao Xiao,<sup>d,e,1</sup> Donglian Xu,<sup>c,a</sup>  
Lei Yang,<sup>b</sup> Ziping Ye,<sup>c</sup> Feiyang Zhang,<sup>a</sup> Tao Zhang,<sup>a,2</sup> Yuanyuan Zhang<sup>a</sup>

<sup>a</sup>*School of Physics and Astronomy, Shanghai Jiao Tong University, MOE Key Laboratory for Particle Astrophysics and Cosmology, Shanghai Key Laboratory for Particle Physics and Cosmology, Shanghai 200240, China*

<sup>b</sup>*School of Electrical Engineering and Intelligent, Dongguan University of Technology, Dongguan 523808, China*

<sup>c</sup>*Tsung-Dao Lee Institute, Shanghai Jiao Tong University, Shanghai 200240, China*

<sup>d</sup>*Department of Physics, University of Maryland, College Park, MD 20742, USA*

<sup>e</sup>*Center of High Energy Physics, Peking University, Beijing 100871, China*

**ABSTRACT:** This paper describes the design and construction of the automatic calibration unit (ACU) for the JUNO experiment. The ACU is a fully automated mechanical system. It is capable of deploying multiple radioactive sources, an ultraviolet (UV) laser source, or an auxiliary sensor such as a temperature sensor, one at a time, into the central detector of JUNO along the central axis. It is designed as a primary tool to precisely calibrate the energy scale of detector, aligning timing for the photosensors, and partially monitoring the position-dependent energy scale variations.

**KEYWORDS:** Detector alignment and calibration methods (lasers, sources, particle-beams); Gamma detectors (scintillators, CZT, HPG, HgI etc); Neutrino detectors

---

<sup>1</sup>Corresponding author, mengjiaoxiao@gmail.com

<sup>2</sup>Corresponding author, tzhang@sjtu.edu.cn

---

## Contents

<b>1</b>	<b>Introduction</b>	<b>1</b>
<b>2</b>	<b>Requirements</b>	<b>2</b>
<b>3</b>	<b>Design of the ACU</b>	<b>3</b>
3.1	Material selection	3
3.2	Mechanical design	3
3.2.1	Turntable	4
3.2.2	Spool for the radioactive source	5
3.2.3	Spool for the UV fiber	6
3.2.4	Spool for the temperature sensor	6
3.2.5	Load cell	9
3.2.6	Cameras	9
3.2.7	Interface to the CD	9
3.3	Electronics and wiring	10
3.3.1	Internal wiring	10
3.3.2	External wiring	11
3.3.3	Groundings	12
3.4	Design of the control software	13
3.5	Safety considerations	15
<b>4</b>	<b>Performance of the ACU</b>	<b>15</b>
4.1	Positioning accuracy	15
4.2	Load cell sensitivity	18
4.3	Exercised safety features	18
<b>5</b>	<b>Summary</b>	<b>19</b>

---

## 1 Introduction

JUNO is an ultra-low background liquid scintillator (LS) detector under construction in the Jiangmen city in south China [1]. At present, the civil construction is mostly completed, and the completion of the detector assembly is expected by the end of 2022. It is designed as a general low background terrestrial and astrophysical neutrino observatory, particularly to perform precision oscillation studies using reactor neutrinos at a baseline of 53 km, in order to determine the neutrino mass hierarchy (MH) [2]. Its central detector (CD) is an acrylic spherical vessel with an inner diameter of 35.4 m, viewed by about 17,600 20-inch and 25,600 3-inch photomultiplier tubes (PMTs) immersed in an ultra-pure water shield [3].

To achieve the MH measurement, the precision of the reactor neutrino spectroscopy has to be better than 1% in energy scale and better than 3% in the effective energy resolution [4]. These in turn pose a great challenge to the detector calibration. In Ref. [5] we described the development of a comprehensive calibration strategy to address the challenge, combining wisdom from past low energy neutrino experiments [6–11]. Several calibration hardware subsystems have been previously reported in Refs. [12–15]. In this paper, we discuss one of the key components of the calibration system, the ACU, envisioned as a primary tool to perform detector calibration on a regular basis.

The paper is organized as follows. In Sec. 2, a brief description is given about the technical requirements of the ACU. The design of the ACU is discussed in Sec. 3. In Sec. 4, we discuss the performance of the as-built ACU, followed by the summary in Sec. 5.

## 2 Requirements

The main purpose of the ACU is to calibrate the energy scale and the position non-uniformity along the central axis to a 0.1% precision at each position, and to calibrate the timing of the PMTs to sub-ns precision. As the most frequently operated calibration subsystem, the technical requirements are:

1. It needs to be extremely reliable, and should be fully automated.
2. It should be able to deploy at least a gamma, or a neutron, or a UV laser light source, one at a time, into the CD along the central axis.
3. For flexibility, an auxiliary device (for example a temperature sensor) with standard connection interface can be easily deployed by the ACU.
4. The positioning accuracy needs to be controlled to less than 1 cm.
5. The ACU should be sealed with the CD to avoid an external radon leak. The total leakage requirement of the ACU is less than  $10^{-5}$  mbar·L/s [16].
6. Calibration sources induced background to the CD should be minimized.
7. Under no circumstances shall a calibration source drop into the CD or damage the CD.
8. The PMT readout should not be affected by electromagnetic noise from the ACU.
9. The ACU control system should be able to communicate with the trigger electronics. For example, if the trigger electronics detects a supernova burst, it should stop the ACU operation immediately.
10. The LS chemical compatibility and cleanliness: all mechanical parts directly or indirectly in contact with the LS must not influence the properties of the LS.
11. Light should not leak into the CD through the ACU.

### 3 Design of the ACU

An illustration of the design of the ACU is shown in Fig. 1, similar to the calibration unit in the Daya Bay experiment [6]. Details of the design features shall be discussed below.

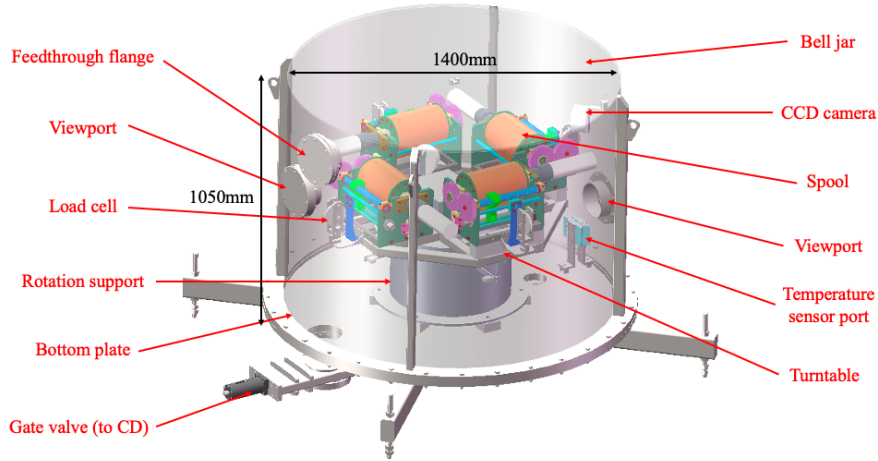


**Figure 1.** An illustration of the design of the ACU.

#### 3.1 Material selection

The JUNO LS is based on linear alkyl benzene (LAB) [17], which is a chemically mild organic liquid. The source and the cable will be in direct contact with the liquid scintillator when deployed into the CD. To avoid adverse long term effect to the LS, especially the optical properties, we perform LS immersion tests on various candidate samples, accelerated in an oven at 40 °C. The absorption spectrum of the liquid is measured before and after the immersion. If the change of the deterioration rate is less than  $10^{-4}$  (after the corrections of surface-to-volume ratios between the aging and experiment conditions, and the accelerated aging lifetime), the material is considered as a good material [18]. Table 1 shows a list of good materials, although some of the materials are only in contact with the vapor of the LS in our system. All commercial components with unknown surfaces are enclosed within these good materials.

To avoid induced radioactivity, the surface cleanliness of the ACU should follow the JUNO cleanliness protocol [19, 20]. Radon emanation from material surface is another concern. Most of the 304 SS surfaces in the ACU are electropolished to a  $1.6 \mu\text{m}$  roughness to reduce emanation. The ACU also contains  $\text{N}_2$  flushing ports to bring out the radon as well as potential oxygen outgassing during the operation, important for the radioactivity control and the light properties of the LS. Moreover, the penetration hole of the ACU bottom plate is sealed from the CD by a normally-closed gate valve.

#### 3.2 Mechanical design

The ACU is enclosed in a stainless steel vacuum sealed bell jar with 1400 mm inner diameter and 1050 mm height (Fig. 2(a)). Two viewports (normally blanked off to avoid light leaks) and one

**Table 1.** Materials used in the ACU.

Materials	components
304 Stainless Steel (SS)	most structural materials, bolts and nuts
Aluminum extrusion	some structural materials
Nickel	temperature sensor parts
Ceramic	balls and bearings
Polytetrafluoroethylene (PTFE)	electric cable jacket, source enclosure, spool
Fluorinated Ethylene Propylene (FEP)	deployment cable jacket
Polyurethane (PU)	electric cable jacket
Acrylic	surface enclosure
Viton	o-rings
Ethylene Tetrafluoroethylene (ETFE)	optical fiber jacket
Loctite epoxy	sealing glue
Polyvinyl Chloride (PVC)	heat shrink tubing
Polyacetal (POM)	spool gear
Polyetheretherketone (PEEK)	bolts

electrical feedthrough flange are on the side wall of the bell jar. The bottom plate of the ACU is 18 mm thick with one electrical feedthrough flange and a 150 mm diameter hole aligning with the central axis of the CD, 620 mm offset from the center of the bottom plate, through which the source can be lowered into the CD. During the regular non-calibration data taking, a gate valve seals the hole from the underside of the bottom plate.

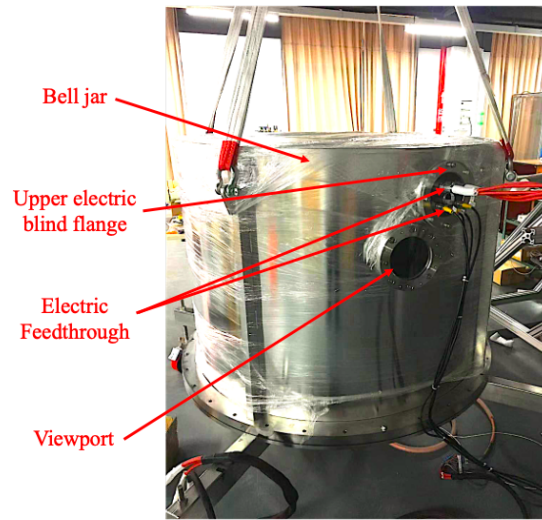
A picture of the complete ACU without the bell jar is shown in Fig. 2(b), we will discuss all of the components in turn.

### 3.2.1 Turntable

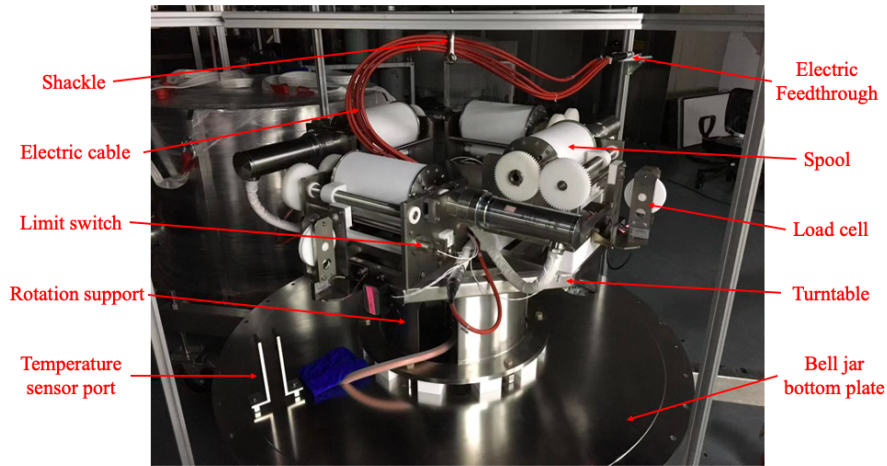
The body inside the ACU is a steel turntable including four mechanically independent motor/spool mechanisms. Each spool is able to deploy a source (a UV fiber with a diffuser ball, a radioactive source, or some auxiliary device which can be attached to the standard source connector) into the CD along the central axis. The four spools are installed with azimuthal separation of  $90^\circ$ , as shown in Fig. 3.

The turntable is capable of turning clockwise or counter-clockwise by a servo motor installed at the center of its supporting structure. The center of each source is radially displaced from the center of the turntable by 620 mm. Once it is aligned with the 150 mm hole at the bottom plate, the source can be deployed into the CD.

Mechanical details of the turntable are illustrated in Fig. 4. A stainless steel rotation support is installed at the center of the bottom plate. The top surface of the rotation support is a U-shaped groove, hosting 40 12.3 mm ceramic balls, evenly distributed by a PTFE retainer. This mechanism serves both as a support to the turntable and the bearing for its rotation. An IP69K watertight servo motor (Kollmorgen AKMH-CNT2GE5K) coupled to a 100:1 gear box (Thomson AQT060-100-0-MMR-724) is installed at the center of the rotation support. The shaft of the gear box couples to the turntable via a flexible bellow coupling (R+W BK8 series). In order to limit the range of the



(a)



(b)

**Figure 2.** (a) Photo of the ACU bell jar; (b) All the ACU components mounted onto the bottom plate.

rotation, two push-button-style stainless steel limit switches (Schurter) are installed on the rotation support to define the limits.

### 3.2.2 Spool for the radioactive source

Fig. 5 illustrates details of a spool for radioactive source deployment. It consists of an IP69K watertight servo motor (Kollmorgen AKMH-CNT2GE5K) coupled to a 10:1 gear box (Thomson AQT060-010-0-MMR-724) and a 160 mm diameter PTFE deployment spool with helical grooves. An FEP-coated flexible 1 mm diameter stainless steel cable is wound in the grooves. The open end of the cable runs through a PTFE pulley, then gets attached to a radioactive source (Fig. 6). When the servo motor drives the spool to unwind the cable, the source can be deployed under gravity into

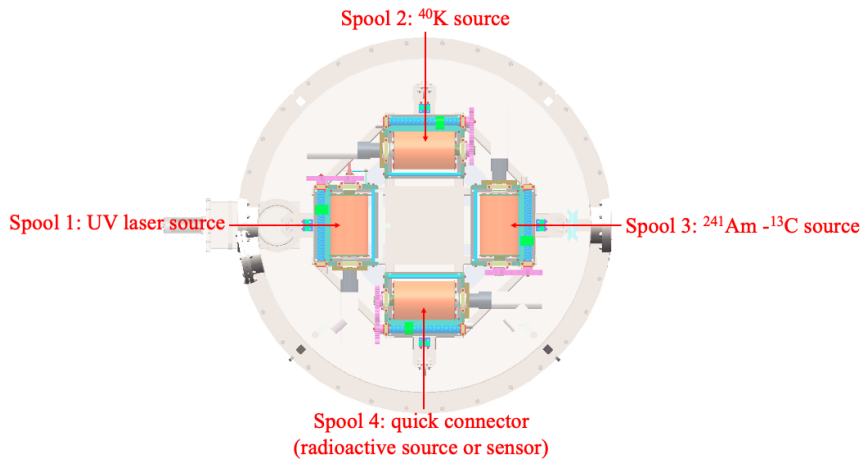


**Figure 3.** Top view of the ACU turntable.

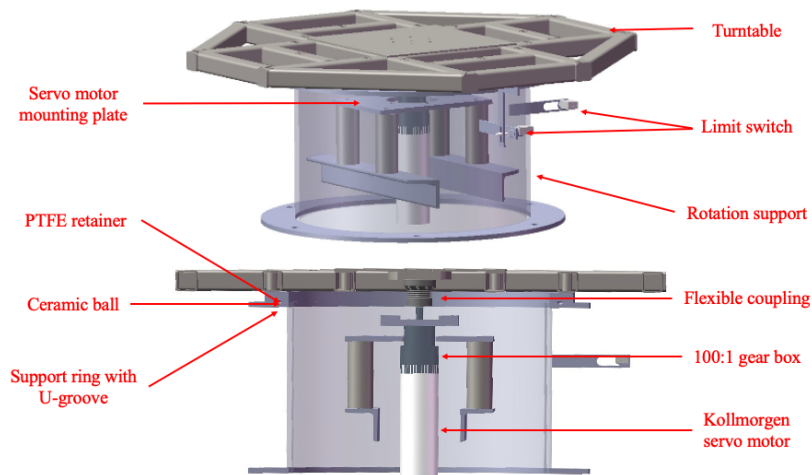


**Figure 4.** Drawings of the turntable.

the CD. To minimize the risk of the cable exiting a groove, a PTFE cable guide driven by two POM gears moves synchronously with the cable. In addition, a PTFE roller press keeps the cable in the grooves. The motion limits are set by two push-button-style stainless steel limit switches (Schurter).

### 3.2.3 Spool for the UV fiber

The design of spool for the UV fiber source is slightly different, as we need to deploy a multi-mode optical fiber to transmit the UV laser light into the CD. Details of this spool can be found in Ref. [21]. An optical fiber rotary joint (MOOG FO228) is connected with the shaft of the spool to link the optical fiber placed outside the ACU bell jar to the fiber rotating with the spool.

### 3.2.4 Spool for the temperature sensor

The fourth spool is envisioned to be flexible. The open end of the cable is attached to a custom connector (see Fig. 7), which is able to attach either an auxiliary sensor or a radioactive source.

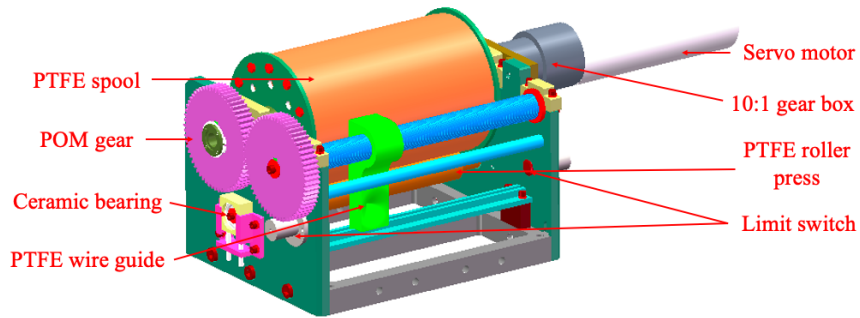


**Figure 5.** Drawing of the radioactive source spool.

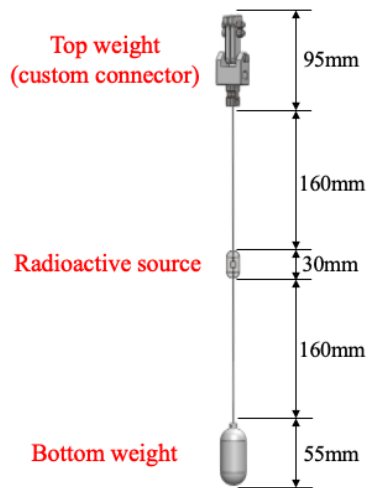


**Figure 6.** A schematic diagram of a radioactive source assembly. A custom connector serves as a top weight. The  $6 \times 6 \text{ mm}^2$  SS radioactive source capsule is enclosed in a PTFE enclosure. A Nickel block enclosed by a PTFE enclosure serves as the bottom weight.

The quick connector consists of a female receptacle and a removable male plug. The plug can be inserted straight into the receptacle. To detach the plug, one has to use a pin tool to push in both tongues then pull to separate. This simple manual operation (although envisioned to be very rare) can be performed by opening the ACU viewport. To be safe, the gate valve should be shut, so this action can be performed even when the JUNO is fully operational.

We designed a watertight wireless temperature sensor to facilitate the measurement of the LS temperature along the central axis. The LS temperature affects the neutron capture time. It also affects the speed of the sound, a key input for the ultrasonic source positioning system [22]. As shown on the left side of Fig. 8, the temperature sensor consists of a three-part shell, each serving as an electrode (from top to bottom:  $V_{in}$ , Data, and Ground), insulated by PEEK rings. The temperature sensor (INNOVATIVE SENSOR TECHNOLOGY TSIC506,  $0.1 \text{ } ^\circ\text{C}$ ), its digital

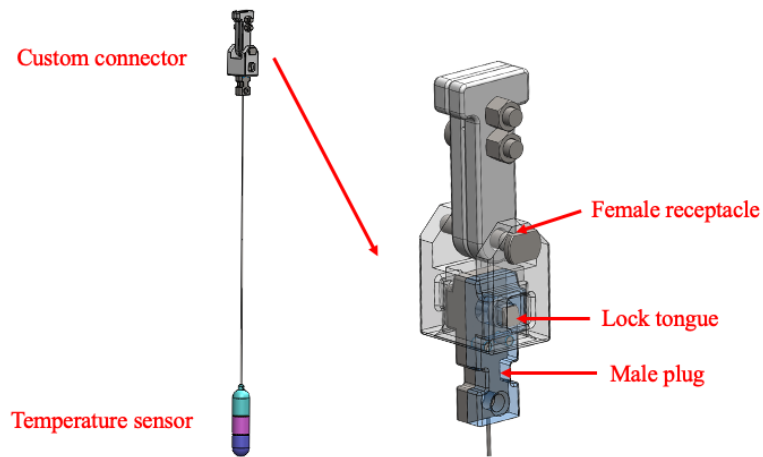


**Figure 7.** A schematic diagram of temperature assembly (left) and the custom connector (right).

readout card, and a rechargeable battery are sealed inside the shell, with the sensor head in tight thermal contact with the lower shell, made with pure Nickel for better thermal conductivity. The temperature data will be stored on the readout board with timestamps during the deployment. Shown on the right side of Fig. 8 is the readout port mounted on the bottom plate, for reading the temperature data and recharging the battery. The port has three pairs of stainless steel spring electrodes to make electrical contact with corresponding pieces on the temperature shell. To read the data, the temperature sensor will be moved directly below the port, and get pulled upward in place. When the wire gets retracted further upward, the sensor gets released from the port to the parking position.

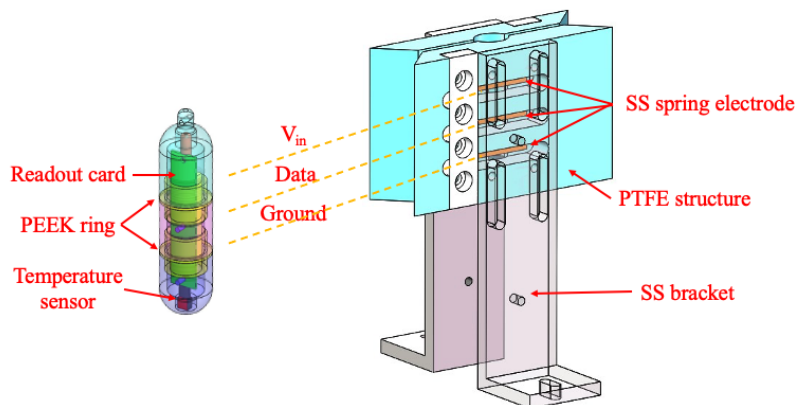


**Figure 8.** Drawing of the temperature sensor and its readout port.

### 3.2.5 Load cell

A PTFE pulley with a ceramic bearing serves as a guide wheel for the calibration cables. A stainless steel S-shape load cell (Longlv LLBLS-I) with a full range of 5 kg and an accuracy 1.5 g, is mounted below the pulley to constantly monitor the tension in the cable (Fig. 9). To set the scale, the weight of the cable is approximately 3 g/m, and that of the entire source assembly is about 200 g. Too much tension may cause damage to the cable or joints, and a loss of tension could result in the cable slipping out of in the grooves of spool.

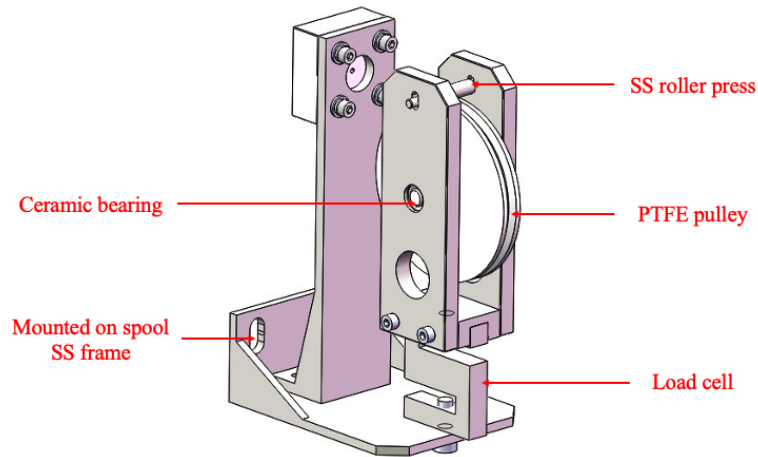


**Figure 9.** Drawing of the load cell.

Because the raw analog outputs of the load cell are of the order of mV, to avoid noise pickup, a digital transducer (SMOWO RW-ST01D 2.1) is used to digitize the signal into RS485 signals before transmission.

### 3.2.6 Cameras

In order to remotely monitor the components inside the ACU, two CCD cameras (HIKVISION DS-2CE16D1T-IT3F) with infrared LED lighting are installed on the inner barrel of the bell jar. Fig. 10 is a picture of the CCD camera in a custom acrylic enclosure. The lighting will be turned off during normal data taking, so it will not affect the CD PMTs. Two images taken by the cameras are shown in Figs. 11(a) and 11(b) when the ACU is kept in the darkness.

### 3.2.7 Interface to the CD

Fig. 12 is a schematic diagram of the ACU interface to the CD. The ACU is installed on the top of the calibration house, where other calibration devices are located. The 150 mm diameter gate valve, through which the sources go in and out of the ACU, is sealed to calibration house through a flexible stainless steel bellow. The bottom of the calibration house seals to a 7.85 m long stainless steel chimney of the CD. Unlike the ACU system in the Daya Bay experiment which sat right on top of the neutrino detector under water [6], the JUNO ACU is installed in the experimental hall,

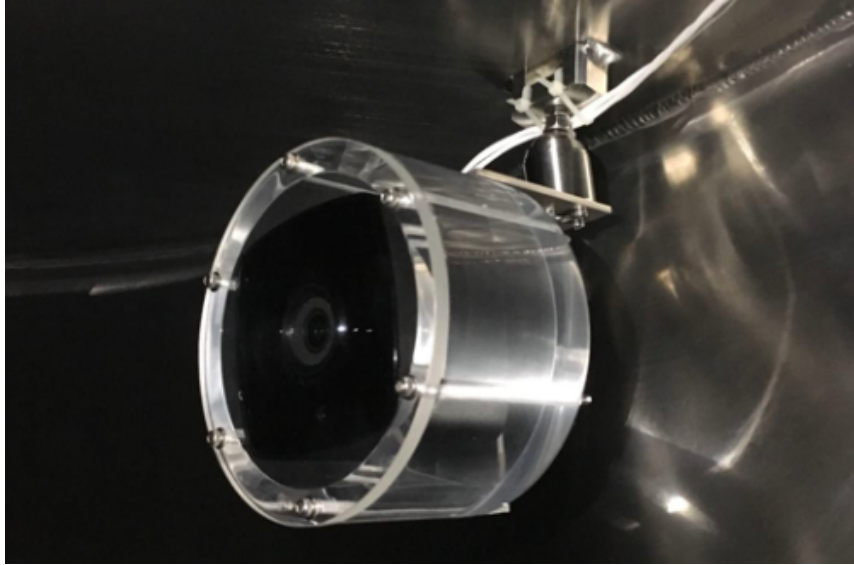


**Figure 10.** Picture of the CCD camera enclosed in an acrylic cylinder.

separated from the CD by the water shielding. The nominal rate for each source is set to be around 100 gamma or neutron emissions per second [5]. Their contribution to the CD rate is limited to less than 1 mHz, according to the simulation. Therefore, no additional shielding inside the ACU is needed.

The bell jar seals to the bottom plate by a double o-ring seal, so that leak check can be performed by pumping the volume between the two o-rings. A Helium sniffer leakage detection technique was used off-site of JUNO in the quality assurance procedure. The upper limit of leakage rate was measured to be  $3 \times 10^{-6}$  mbar·L/s.

### **3.3 Electronics and wiring**

#### **3.3.1 Internal wiring**

A schematic diagram of the ACU's overall wiring scheme is shown in Fig. 13.

Two 48-pin feedthroughs (LEMO SGJ4B348CLMPV) and four isolated BNC feedthroughs (MPF A0466-4-W) are mounted on an ISO-160 vacuum flange (upper electric flange). The two 48-pin feedthroughs are used for connections of the components on the turntable. Two of the BNC connections carry the 12 V power supply for each CCD cameras, and the other two carry the image signals. The feedbacks of the servo motors, and the load cell power supplies and signals get collected by a breakout board located inside a shielded stainless steel box on the turntable. To avoid crosstalk between the power and feedback of the servo motors, their power lines and limit switches get consolidated by the other breakout board, shielded from the first one. Through multiple twist-pair cables, each breakout board connects to a 48-pin female connectors (LEMO FGG4B348CLAD15 and FGJ4B348CLAD15), mating to the feedthroughs on the upper electric flange. All twisted-pair cables go upward through a rotatable shackle from the center of the bell jar dome, then run horizontally to connect to the upper electric flange. This ensures that cables will not run into other components while the turntable is rotating.



(a)



(b)

**Figure 11.** Images of the interior of the ACU taken by the two CCD cameras.

One 30-pin feedthrough (LEMO SGJ4B330CLMPV) is mounted on an ISO-100 vacuum flange (lower electric flange), connecting to the turntable servo motor, its limit switches, and the temperature sensor port.

### 3.3.2 External wiring

Outside the ACU, the cables (~10 m) go all the way from the upper and lower electric flanges to the control box located on the platform below the calibration house (Fig. 12). The wiring is also indicated in Fig. 13.

A diagram and picture of the ACU control box are shown in Figs. 14(a) and 14(b). It consists of five servo drivers for the spool and turntable servo motors, a programmable logic controller (PLC) (YOKOGAWA), one 12 V power supply for temperature sensor port and CCD cameras, and two 24 V power supplies for load cell transducers and servo drivers. The motion control, data

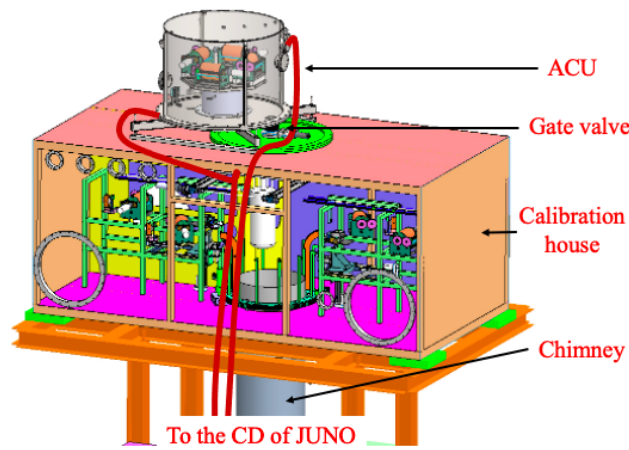


**Figure 12.** A schematic diagram of the ACU interface to the CD.

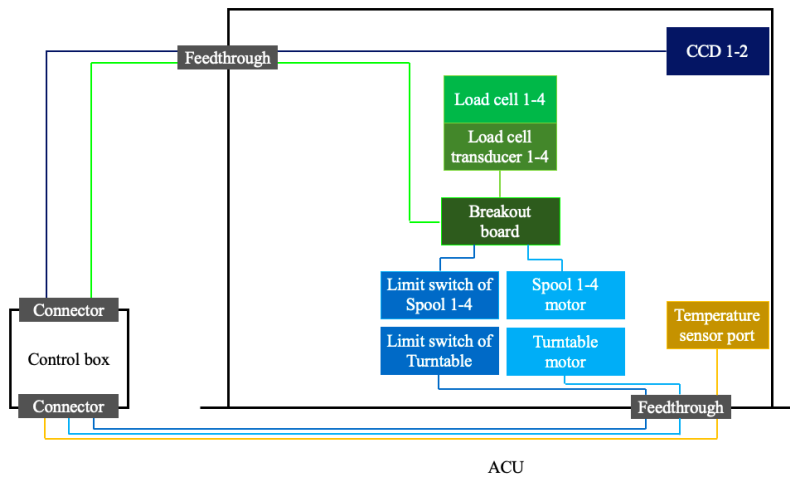


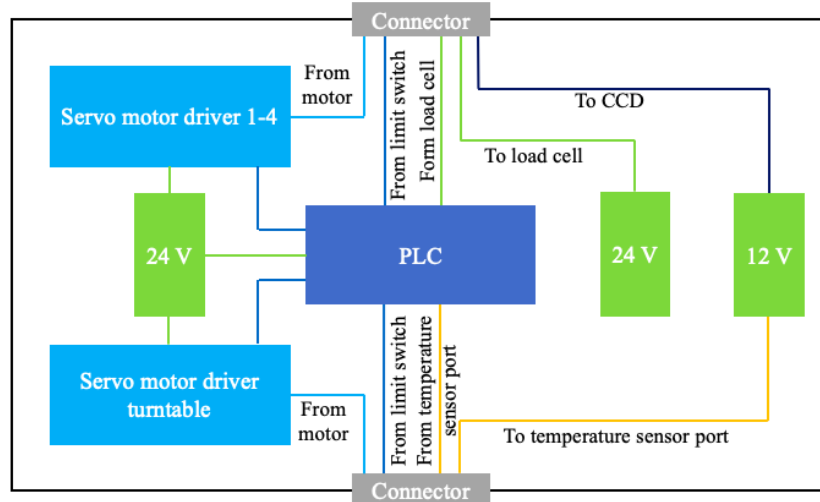
**Figure 13.** A schematic diagram of the ACU wiring scheme.

acquisition, and communications are all controlled by the PLC. To avoid servo motors introducing noises in the CD, relays are implemented in the control box to remotely disable the servo drivers, etc., when the sources are not moving.

The power line of the control box is drawn from the main AC 220 V power from the electronics room to allow single point grounding. The PLC in the control box is connected via an Ethernet cable to a Windows 10 computer located in the electronics room, serving as a state monitor.

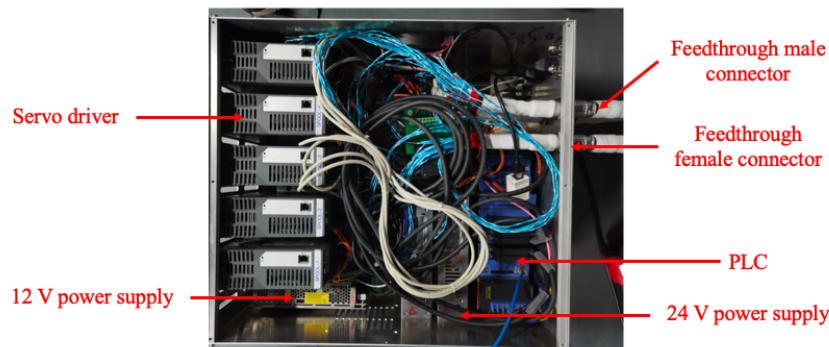
### 3.3.3 Groundings

JUNO has two independent power and ground systems: so-called the "clean" and "dirty". The PMT and its electronics system run on the clean power and clean ground, whereas most of the utilities run on the dirty power and safety ground. Since the ACU uses motors, by default, the ACU will be



Control box

(a)



(b)

**Figure 14.** A diagram (a) and a picture (b) of the ACU control box.

connected to the dirty power. On the other hand, most CD structure will be on the clean ground, therefore it is imperative that the electronics components inside the ACU be completely insulated from the bottom plate. To achieve this, the rotation support is insulated from the bottom plate by PTFE spacers and PEEK bolts, as illustrated in Fig. 15.

### 3.4 Design of the control software

The design of the ACU control software follows two guidelines: 1) safety, i.e. it should be reliable to interrupt motions immediately when abnormal conditions are detected; and 2) automation, i.e. the calibration sequence is carried out completely without human intervention. The control software is developed in a ladder diagram (the programming language of the PLC), illustrated in Fig. 16, which consists of five application modules: motion control, monitoring, notification, communication, and auxiliary modules. An entire execution cycle was found to take less than 0.1 s. The motion control module controls the five axes (1-4 for the spools and 5 for the turntable) of motion. In the standard

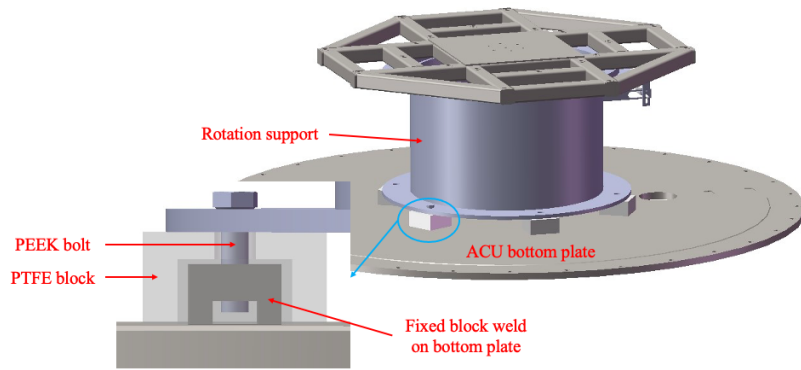


**Figure 15.** The ACU electronics insulation plan.

operation, it reads an XML script which specifies the sequence and detailed parameters of operations to be performed. The monitor module reads data from all sensors. When the values of these sensor exceed prescribed values, the motion control module will stop all motions and the corresponding alarms will appear. The alarms will be broadcast by the notification module. The auxiliary module controls the switches of the CCD cameras and communicates with the temperature sensor port. The communication module talks to the slow control system and the trigger electronics, particularly during the calibration data taking. In addition, when the trigger electronics detects something interesting in realtime (e.g. supernova neutrino burst), the trigger electronics handshakes with the communication module which issues halt signals to all motors.

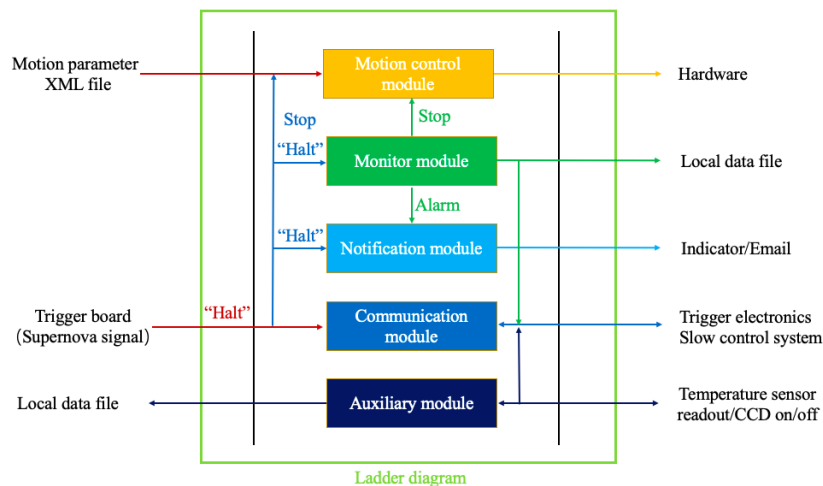


**Figure 16.** The ladder diagram of the ACU control software.

### 3.5 Safety considerations

Robustness of the ACU against possible failures is of ultimate importance. Similar to the design of another calibration subsystem in Ref. [12], the safety considerations implemented in the ACU control are summarized below.

1. All motions are relatively slow. The turntable rotates at a speed of  $2.25^\circ/\text{s}$ , and the sources are deployed at a speed of 15 mm/s. This not only gives reaction time if something goes wrong, but also improves the longevity of servo motor operations.
2. The servo motors used in the ACU are equipped with electromagnetic brakes which will lock the motors during power failure.
3. The rotation angle of the turntable is limited to  $275^\circ$  by two limit switches to avoid over-twisting of electric cables and the laser fiber. The deployment of the spool is also limited by two limit switches to avoid motion beyond allowed range.
4. Each radioactive source assembly contains a top weight and bottom weight above and below the source to maintain the tension in the cable. The double-weight ensures sufficient tension even if the bottom one is touching some obstacle from below.
5. The tension in the deployment cable is constantly being monitored by the load cell to avoid too much or too little tension when the source is stuck or bottomed out.
6. The source enclosure and weights are round-headed to avoid the source getting stuck or damaging the surface that it scrapes on.
7. The breaking strength for the FEP-coated stainless steel cable is about 60 kg. In order to avoid the cable breakage due to the load cell failure, the torque of the servo motor is limited to provide a maximum tension of less than 10 N in the cable. The control software will monitor the current of the servo motor in real time, and shut down the motor when there is excessive current. The same current interlock is also implemented in the turntable motor.
8. The PLC has an internal battery, to allow data to continue being buffered during a power failure.

## 4 Performance of the ACU

A complete ACU has been constructed according to the above design. Rigorous functionality tests have been carried out together with the control software, yielding satisfactory performance in all aspects.

### 4.1 Positioning accuracy

The source deployment position is determined based on two assumptions. First, the cable is within the elastic limit under the typical load of a few hundred grams, so the fractional elongation under gravity is a constant. This assumption has been validated by having two cables of 24 and 35 m hung

vertically with a weight varying from 0 to 300 g repeatedly. Good elasticity has been observed, and under the 200 g source load, the elongation was measured to be  $1.0 \times 10^{-4}$  at 35 m. Even at the maximum length, the elongation is limited to be 5 mm. This can be conservatively taken as an uncertainty. Furthermore, the potential curls in the deployment cable might introduce additional positioning uncertainty in the horizontal plane. After the detector is assembled, we will use the four spools to deploy different sources to the same nominal location, and use the auxiliary CCD cameras [23] (4 mm relative positioning accuracy) to check the position repeatability. Second, the spool diameter is a constant which relates the unwound cable length and the spool rotation as

$$L = \theta/2 \times D + \Delta_0 - \Delta(\theta), \quad (4.1)$$

in which  $\theta$  is the spool rotation in radian,  $D$  is the effective diameter of the spool, and  $\Delta_0$  and  $\Delta(\theta)$  are illustrated in Fig. 17, calculable based on simple trigonometry. Systematic uncertainties can arise due to machining precision of the grooves and how well the cable fits inside the grooves. To study this, for each spool, we unwind and stop the spool every five cycles, and record the cable length using a custom length recorder, which was calibrated against a 9 m tape measure to a precision of 1 mm. Then using Eqn. 4.1, the spool diameter  $D$  is fitted as a floating parameter. To test the positional bias, we then unwind the spool again at 1, 5, 10, 15, 20, 25, 30, 35, 40, 45, and 50 m according to Eqn. 4.1, then measure directly the cable length using the length recorder. The differences between the measurements and expectations vs. distance are summarized in Fig. 18 for the four spools. The yellow band indicates the accumulated systematic uncertainty of the length recorder. Since most of the data points are inside the band, and the largest difference is 5.2 mm (spool 4) at 50 m, we conclude that the uncertainty due to the spool rotation is controlled to be less than 5 mm. In combination with an independent uncertainty due to cable elongation (5 mm), the total vertical position uncertainty is estimated to be 7 mm.

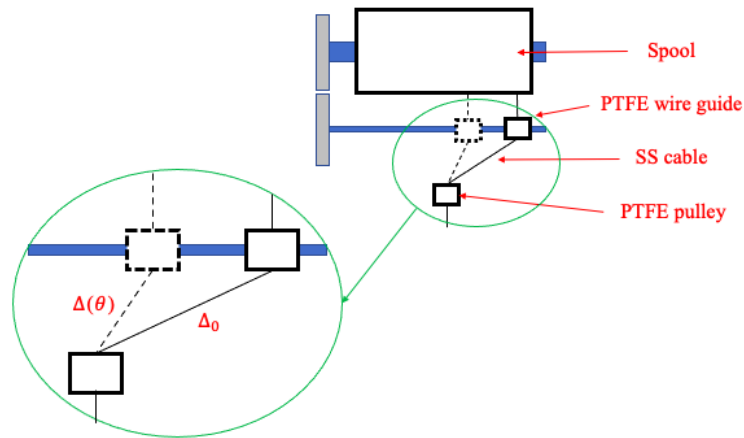


**Figure 17.** An illustration of  $\Delta_0$  and  $\Delta(\theta)$ .

Another ingredient of the positional precision is in the horizontal plane. To deploy a given source, the turntable needs to be rotated to a specified position. Although the precision of the

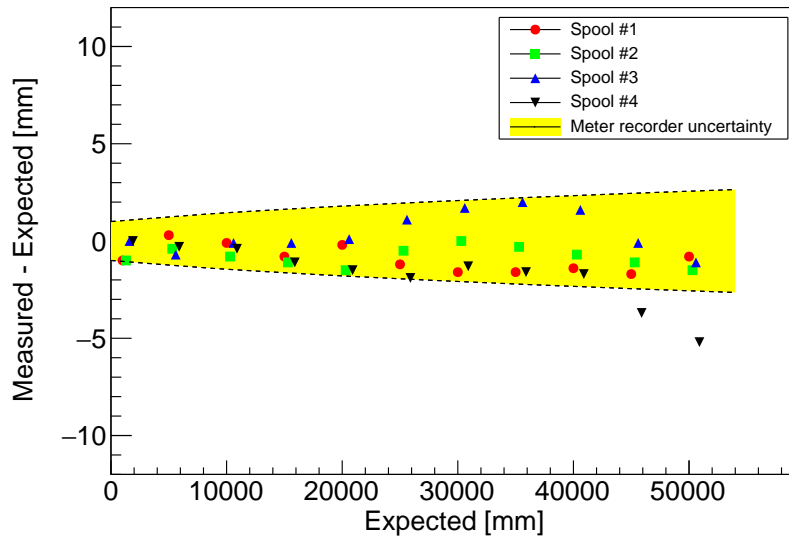


**Figure 18.** Biases in deployed cable length (measured-expected) vs. expected distance for all spools, with color coding indicated in the legend. The yellow band indicates the expected uncertainty of the length measured by the meter recorder.

servo motor and gear rotation is very high, the zero position of the turntable bears non-negligible uncertainty due to the spring actuation of the limit switch. To study this, the turntable is continuously moved back and forth between the zero and  $270^\circ$  60 times, each time resetting zero by hitting the limit switch, then stopping at  $270^\circ$ . The angle between the stopped position and a reference plate is measured by a dial indicator, shown in Fig. 19. The standard deviation of the angle, translated to a horizontal position uncertainty at a radius of 620 mm (the eccentricity of the deployment hole) is 1.1 mm.

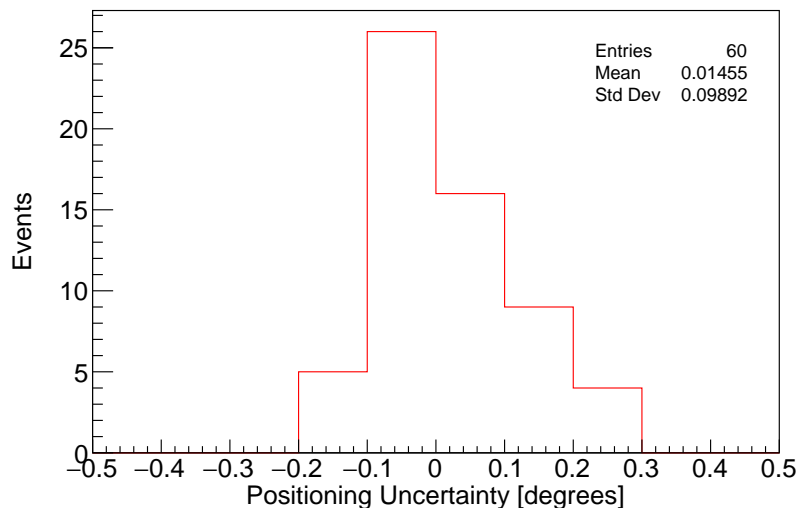


**Figure 19.** The measured angular uncertainty of the turntable.

**Table 2.** The ACU control software safety measure tests.

test item	test method	test result
motion interlock	> 1 servo motor running	all motions stopped, and alarm issued
turntable limit switch	triggered by hand	same as above
spool limit switch	triggered by hand	same as above
load cell	out of range	same as above
servo motor current	out of range	same as above
power outage	power cycle by hand	all motion stopped, electromagnetic brake on, and all data recovered after power cycle

## 4.2 Load cell sensitivity

The load cell is tested with a dummy source deployed from the air into the LS, with its reading depicted in Fig. 20. The change of the tension due to different buoyancy conditions as well as a "bottom-out" situation can be clearly observed. After the source completely leaves the LS, the tension has another slight decrease as the LS initially attached to the source drips back into the liquid, demonstrating the sensitivity of the load cell.

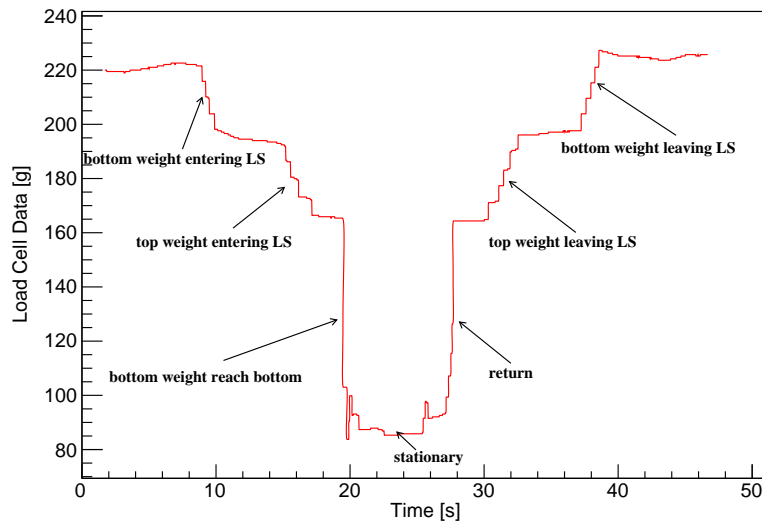


**Figure 20.** Load cell reading for a test deployment of a dummy source into and out of the LS.

## 4.3 Exercised safety features

We have also made repeated tests on all safety measures in the control software. The test results are summarized in Table 2.

## **5 Summary**

In this paper we described the design of the automatic calibration unit for the JUNO experiment, which is capable of deploying multiple radioactive sources, a UV laser source, or an auxiliary sensor along the central axis of the JUNO CD with positional precision better than 1 cm. Long term reliability has been built into the hardware and software design. The production version of the ACU is constructed with its performance tested successfully through a rigorous test program. The ACU will serve as a most frequently used calibration device to meet the challenging physics requirements of JUNO.

## **Acknowledgments**

This work is supported by the Strategic Priority Research Program of the Chinese Academy of Sciences, Grant No. XDA10010800, and the CAS Center for Excellence in Particle Physics (CCEPP). We are thankful for the support from the Office of Science and Technology, Shanghai Municipal Government (Grant No. 16DZ2260200), and the support from the Key Laboratory for Particle Physics, Astrophysics and Cosmology, Ministry of Education.

## References

- [1] T. Adam et al., JUNO conceptual design report, *arXiv:1508.07166*.
- [2] Y.-F. Li, J. Cao, Y. Wang and L. Zhan, Unambiguous determination of the neutrino mass hierarchy using reactor neutrinos, *Phys. Rev. D* 88 (2013) 013008 [arXiv:1303.6733v2].
- [3] F. An et al, Neutrino Physics with JUNO, *J. Physics. G: Nucl. Part. Phys.* 43 (2016) 030401.
- [4] L. Zhan, Y. Wang, J. Cao and L. Wen, Experimental requirements to determine the neutrino mass hierarchy using reactor neutrinos, *Phys. Rev. D* 79 (2009) 073007.
- [5] A. Abusleme et al., Calibration strategy of the JUNO experiment, *JHEP* 03 (2021) 004 [arXiv:2011.06405v3].
- [6] J. Liu et al., Automated calibration system for a high-precision measurement of neutrino mixing angle  $\theta_{13}$  with the Daya Bay antineutrino detectors, *Nucl. Instrum. Meth. A*, 750 (2014) 19-37 [arXiv:1305.2248].
- [7] KamLAND Collaboration, The KamLAND full-volume calibration system, *JINST*, 4 (2009) P04017 [arXiv:0903.0441v1].
- [8] M. R. Dragowsky, Sudbury Neutrino Observatory energy calibration using gamma-ray sources /, *A DISSERTATION submitted to Oregon State University*, (1999).
- [9] B. Caccianiga and A. C. Re, The calibration system for the Borexino experiment, *Int. J. Mod. Phys. A*, 29 (2014) 1442010.
- [10] K. Abe et al., Calibration of the Super-Kamiokande Detector, *Nucl. Instrum. Meth. A* 737 (2014) 253 [arXiv:1307.0162].
- [11] I. Ostrovskiy, Double Chooz Calibration, *Nucl. Phys. B* 229-232 (2012) 431.
- [12] Y. Zhang et al., Cable Loop Calibration System for Jiangmen Underground Neutrino Observatory, *Accepted by NIMA* [arXiv:2011.02183v2].
- [13] Yuhang Guo et al., Design of the Guide Tube Calibration System for the JUNO experiment, *JINST* 14 (2019) T09005 [arXiv:1905.02077v1].
- [14] Yuhang Guo et al., Construction and Simulation Bias Study of GTCS for JUNO, *manuscript in preparation*.
- [15] K. Feng et al., A novel remotely operated vehicle as the calibration system in JUNO, *JINST* 13 (2018) T12001.
- [16] J. Liu private communication.
- [17] Daya Bay Collaboration, JUNO Collaboration, Optimization of the JUNO liquid scintillator composition using a Daya Bay antineutrino detector, *Nucl. Instrum. Meth. A* 988 (2021) 164823 [arXiv:2007.00314v1].
- [18] M. Yeh et al. private communication.
- [19] L. Zhou et al., *Radioactive Cleanliness Control for the JUNO Experiment*, poster at NEUTRINO2020.
- [20] Y. Meng private communication.
- [21] Y. Zhang et al., Laser calibration system in JUNO, *JINST*, 14 (2019) P01009 [arXiv:1811.00354v4].
- [22] G. Zhu et al., Ultrasonic positioning system for the calibration of central detector, *Nucl. Sci. Tech.*, 30 (2019) 5.

[23] A. Abusleme et al., JUNO Physics and Detector, *arXiv:2104.02565v2*.